Chapter 11
Anisotropic Creep Analysis of Fiber Reinforced Load Point Support Structures for Thermoplastic Sandwich Panels

Jörg Hohe and Sascha Fliegener

Abstract The present contribution is concerned with a numerical analysis of creep in load point support structures for sandwich panels made from different fiber reinforced thermoplastic materials. Whereas the face sheets consist of laminates of unidirectional carbon fiber reinforced plies, the support structures for the load points consist of discontinuously long fiber reinforced thermoplastics manufactured in a compression molding process. The sandwich core is a thermoplastic foam. For the numerical creep analysis of such structures under long-term loading, an anisotropic viscoelastic material model is formulated. In different versions, the model is applicable either to unreinforced thermoplastics, or to thermoplastics with discontinuous or continuous fiber reinforcement. The material model is implemented into a finite element system. The model is validated against an experimental data base on both, coupon and structural level.

11.1 Introduction

Structural sandwich panels are found in a variety of technological fields where extreme lightweight solutions are required. In addition to the classical fields of aerospace industry or the wind energy sector, sandwich structures become increasingly popular in transport applications for both the rail and road sector. In contrast to aerospace components with limited numbers of components to be manufactured, especially the automotive sector is characterized by industrial scale mass production with large numbers of components to be manufactured with an extreme demand for short cycle times. For this purpose, polymeric composite and sandwich components consisting of thermoplastic base materials are popular materials for future composite automotive designs (Bijsterbosch and Gaymans [1], Henning et al. [2]). On the other hand, one of

Jörg Hohe · Sascha Fliegener
Fraunhofer-Institut für Werkstoffmechanik IWM, Wöhlerstr. 11, 79108 Freiburg, Germany,
e-mail: joerg.hohe@iwm.fraunhofer.de, sascha.fliegener@iwm.fraunhofer.de

H. Altenbach and K. Naumenko (eds.), *Creep in Structures VI*,
Advanced Structured Materials 194, https://doi.org/10.1007/978-3-031-39070-8_11

the major shortcomings of thermoplastic materials is their inherent tendency towards creep deformation even for discontinuously and in some cases also continuously fiber reinforced microstructures (Chevali et al. [3], Greco et al. [4], Brinson and Knauss [5]).

Objective of the present contribution is the evaluation of load point support structures for thermoplastic sandwich panels, involving hybrid designs of discontinuously and continuously fiber reinforced polymer matrix composites. For this purpose, creep material models for anisotropic fiber reinforced materials are developed and implemented. Based on a classical three term Kelvin-Voigt approach, a preliminary isotropic viscoelastic material model is formulated. Using a Schapery [6] type extension, a stress dependence is implemented. The isotropic base model is extended to anisotropic fiber reinforced materials in a twofold manner. For discontinuously long fiber reinforced materials, a simple generalization based on anisotropy factors is employed. To account for creep effects in continuously unidirectionally fiber reinforced materials, the isotropic base model is superimposed with an isotropic Hooke's law. In this context, the isotropic viscoelastic part represents the matrix response whereas the rate independent anisotropic Hooke's law with (almost) vanishing stiffness perpendicular to the fibers represents the response of the unidirectionally oriented continuous fibers. The different models are implemented as user-defined material models into a commercial finite element program.

In a first application, the numerical approach is validated against experimental data obtained in unidirectional coupon experiments considering unreinforced thermoplastic materials as well as discontinuously and continuously fiber reinforced materials, both tested in different spatial directions. In a second step, the model is applied to load point support structures for sandwich panels made from compression molded long fiber reinforced thermoplastics designed in a previous contribution (Fliegener et al. [7]). The sandwich face sheets are made from multidirectional laminates consisting of unidirectional carbon fiber reinforced thermoplastic plies bonded to a thermoplastic foam core. The results of the simulations are validated against experimental data obtained in creep experiments. The numerical predictions are found in good agreement with the experimental observations.

11.2 Material Model

The analyses in the present study employ the material models presented by the authors in an earlier contribution (Fliegener and Hohe [8]). Therefore, only a brief outline is given here.

11.2.1 Basic One-Dimensional Formulation

The model is based on a three element Kelvin-Voigt model using the rheological model sketched in Fig. 11.1. For this type of model the one-dimensional time dependent strains are given by the convolution integral

$$\varepsilon(t) = \int_0^t \left(\frac{1}{E^{(0)}} + \sum_{q=1}^{3} \frac{1}{E^{(q)}} \left(1 - e^{-\frac{t-t^*}{\tau^{(q)}}} \right) \right) \frac{\partial \sigma}{\partial t} \bigg|_{t=t^*} \mathrm{d}t^* \tag{11.1}$$

where where the elastic moduli $E^{(q)}$ and the relaxation times

$$\tau^{(q)} = \frac{\eta^{(q)}}{E^{(q)}} \tag{11.2}$$

together with the viscosities $\eta^{(q)}$ are material parameters.

Transforming Eq.(11.1) into a strain dependent incremental form results in

$$\mathrm{d}\sigma(t) = \tilde{E}(t) \left(\mathrm{d}\varepsilon(t) - \sum_{q=1}^{3} \left(1 - e^{-\frac{\mathrm{d}t}{\tau^{(q)}}} \right) \varepsilon^{\mathrm{i}(q)}(t - \mathrm{d}t) \right) \tag{11.3}$$

with the time dependent tangential stiffness

$$\tilde{E}(t) = \left(\frac{1}{E^{(0)}} + \sum_{q=1}^{3} \frac{1}{E^{(q)}} \left(1 - \frac{\tau^{(q)}}{\mathrm{d}t} \left(1 - e^{-\frac{\mathrm{d}t}{\tau^{(q)}}} \right) \right) \right)^{-1} \tag{11.4}$$

and the inherited strains $\varepsilon^{\mathrm{i}(q)}$ defined in a recursive manner by

$$\mathrm{d}\varepsilon^{\mathrm{i}(q)}(t) = \left(\frac{\tau^{(q)}}{E^{(q)}} \frac{\partial \sigma}{\partial t} - \varepsilon^{\mathrm{i}(q)}(t - \mathrm{d}t) \right) \left(1 - e^{-\frac{\mathrm{d}t}{\tau^{(q)}}} \right) \tag{11.5}$$

forming history variables.

Linear viscoelstic models are in many cases inadequate to model the time dependent stress-strain response observed in experiments (e.g. Fliegener et al. [9], Haj-Ali and Muliana [10], Schapery [6]). For this reason, the parameters $E^{(q)}$ in Eqns. (11.4) and (11.5) are considered as stress dependent functions $E^{(q)}(\sigma)$ rather than constant moduli. Full details on the employed material model and its definition can be found in the original contribution (Fliegener and Hohe [8]).

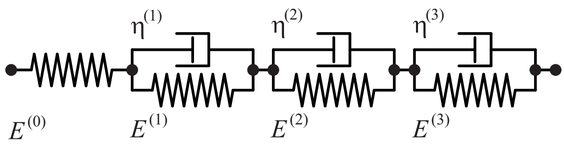

Fig. 11.1 Three element Kelvin-Voigt model.

11.2.2 Generalization to Three Dimensions

The one-dimensional viscoelastic material model (11.3) is generalized to the three-dimensional space in the same manner as Hooke's law since it must reduce to Hooke's law, if all viscous parts are deactivated by an appropriate choice of the material parameters. Therefore, the material model (11.3) is decomposed into a volumetric and a deviatoric part, resulting in the three-dimensional form

$$\begin{aligned} \mathrm{d}\sigma_{ij}(t) = 2\tilde{G}(t)\left(\mathrm{d}\varepsilon'_{ij}(t) - \sum_{q=1}^{3}\left(1-e^{-\frac{\mathrm{d}t}{\tau^{(q)}}}\right)\varepsilon_{ij}^{\mathrm{is}(q)}(t-\mathrm{d}t)\right) \\ +3\tilde{\kappa}(t)\left(\mathrm{d}\varepsilon^{\mathrm{v}}(t) - \sum_{q=1}^{3}\left(1-e^{-\frac{\mathrm{d}t}{\tau^{(q)}}}\right)\varepsilon^{\mathrm{iv}(q)}(t-\mathrm{d}t)\right)\delta_{ij} \end{aligned} \tag{11.6}$$

with the time-dependent shear and bulk stiffnesses

$$\tilde{G}(t) = \left(\frac{1}{G^{(0)}} + \sum_{q=1}^{3}\frac{1}{G^{(q)}}\left(1-\frac{\tau^{(q)}}{\mathrm{d}t}\left(1-e^{-\frac{\mathrm{d}t}{\tau^{(q)}}}\right)\right)\right)^{-1} \tag{11.7}$$

$$\tilde{\kappa}(t) = \left(\frac{1}{\kappa^{(0)}} + \sum_{q=1}^{3}\frac{1}{\kappa^{(q)}}\left(1-\frac{\tau^{(q)}}{\mathrm{d}t}\left(1-e^{-\frac{\mathrm{d}t}{\tau^{(q)}}}\right)\right)\right)^{-1} \tag{11.8}$$

respectively. The generalized bulk and shear moduli are defined by

$$G^{(q)} = \frac{E^{(q)}}{2(1+\nu)} \tag{11.9}$$

$$\kappa^{(q)} = \frac{E^{(q)}}{3(1-2\nu)} \tag{11.10}$$

in the same manner as for Hooke's law. The Poisson's ratio ν is assumed to be a material constant, which is not affected by viscoelasticity. The evolution equation (11.5) is generalized to the three-dimensional case by

$$\mathrm{d}\varepsilon_{ij}^{\mathrm{is}(q)}(t) = \frac{1}{\tilde{G}(t)}\frac{\tau^{(q)}}{\mathrm{d}t}\left(1-e^{-\frac{\mathrm{d}t}{\tau^{(q)}}}\right)\mathrm{d}\sigma'_{ij} - \varepsilon_{ij}^{\mathrm{is}(q)}(t-\mathrm{d}t)\left(1-e^{-\frac{\mathrm{d}t}{\tau^{(q)}}}\right) \tag{11.11}$$

$$\mathrm{d}\varepsilon^{\mathrm{iv}(q)}(t) = \frac{1}{\tilde{\kappa}(t)}\frac{\tau^{(q)}}{\mathrm{d}t}\left(1-e^{-\frac{\mathrm{d}t}{\tau^{(q)}}}\right)\frac{\mathrm{d}\sigma_{kk}}{3} - \varepsilon^{\mathrm{iv}(q)}(t-\mathrm{d}t)\left(1-e^{-\frac{\mathrm{d}t}{\tau^{(q)}}}\right) \tag{11.12}$$

where the history variables $\varepsilon_{ij}^{\mathrm{is}(q)}$ and $\varepsilon^{\mathrm{iv}(q)}$ are the deviatoriv and volumetric inherited strains, respectively.

11.2.3 Unidirectionally Fiber Reinforced Thermoplastics

The three-dimensional constitutive equation (11.6) constitutes an isotropic viscoelastic material law. For fiber reinforced materials, this model needs to be generalized to cover anisotropic material response as well.

For the case of a continuous unidirectional fiber reinforcement, it is assumed that stresses deriving from the deformation of the isotropic viscoelastic matrix and stresses deriving form the deformation of the linear elastic anisotropic fiber reinforcement can be superimposed by

$$d\sigma_{ij} = (1-\rho^{\mathrm{f}})d\sigma_{ij}^{\mathrm{m}} + \rho^{\mathrm{f}} d\sigma_{ij}^{\mathrm{f}} \tag{11.13}$$

where $d\sigma_{ij}^{\mathrm{m}}$ are the stress increments in the matrix determined by Eq. (11.6) whereas the fiber stress increments

$$d\sigma_{ij}^{\mathrm{f}} = C_{ijkl}\varepsilon_{kl} \tag{11.14}$$

are obtained by means of the anisotropic Hooke's law considering the anisotropic stiffness induced to the composite by the fiber reinforcement. The parameter ρ^{f} denotes the fiber volume fraction.

11.2.4 Discontinuously Fiber Reinforced Thermoplastics

For the case of a discontinuous multidirectional fiber reinforcement, the effect of the anisotropy of the composite is modelled in a pragmatic manner by introduction of weight factors into the equations for the normal stresses in the different spatial directions. For this purpose, Eq. (11.6) is substituted with

$$\begin{aligned} d\sigma_{ij}(t) = 2\tilde{G}(t)&\left(\bar{s}^{\mathrm{d}} d\varepsilon'_{ij}(t) - \sum_{q=1}^{3}\left(1-e^{-\frac{dt}{\tau^{(q)}}}\right)\varepsilon_{ij}^{\mathrm{is}(q)}(t-dt)\right) \\ +3\tilde{\kappa}(t)&\left(\bar{s}^{\mathrm{v}} d\varepsilon^{\mathrm{v}}(t) - \sum_{q=1}^{3}\left(1-e^{-\frac{dt}{\tau^{(q)}}}\right)\varepsilon^{\mathrm{iv}(q)}(t-dt)\right)\delta_{ij} \end{aligned} \tag{11.15}$$

where the weight factors

$$\bar{s}^{\mathrm{d}} = \begin{cases} s^{\mathrm{d}} & \text{if } : i = j = 1 \\ 1 & \text{else} \end{cases} \tag{11.16}$$

$$\bar{s}^{\mathrm{v}} = \begin{cases} s^{\mathrm{v}} & \text{if } : i = j = 1 \\ 1 & \text{else} \end{cases} \tag{11.17}$$

are factors used to introduce a proces and fiber preference orientation related anisotropy of the material response. Both factors may be dependent on the flow characteristics of the material during molding or other process parameters and thus will – in general – depend on the spatial position in the final component. Full details and a broader discussion on the formulation of the constitutive model are given in the original contribution (Fliegener and Hohe [8]).

The proposed material model for all three material types – neat isotropic polymeric material as well as anisotropic continuously and discontinuously fiber reinforced materials – are implemented as user defined materials into a commercial finite element code.

11.3 Experimental Investigation

The theoretical developments of the material model in Sect. 11.2 are complemented by an experimental investigation to provide a data base for validation and demonstration of its capabilities. Creep tests are performed on both coupon and structural level.

11.3.1 Coupon Experiments

For determination of the material parameters for the different levels of the creep model proposed in Sect. 11.2 and for a first validation, creep experiments on coupon level are performed. Three different grades of material are investigated, each supplied with a polyamide (PA) 6 matrix. The first grade is the neat matrix material. The second grade is a long glass fiber reinforced (LFT) material manufactured in a compression molding process. The material is supplied with fiber weight and volume fractions of 40wt.% and 22.5vol%, respectively. The third material grade is a unidirectionally (UD) carbon fiber reinforced material with a fiber volume fraction of 46vol%. The material was processed by Fraunhofer ICT and BASF and supplied in form of plane plates.

From the available plates, coupon specimens are manufactured using waterjet cutting. For the neat matrix material as well as for the LFT material and the UD material to be tested perpendicular to the fiber direction, dogbone specimens according to ISO 3167 [11], type A are used, supplied with an increased shoulder radius of 50 mm and – due to limited material availability – for the neat matrix material with a reduced gauge section length of 36 mm. For the UD materal to be tested within the fiber direction, straight specimens according to ISO 527-5 [12], type A with an increased width of 20 mm are used.

The specimens are tested for their creep response under tensile loads according to ISO 899-1 [13] using a dead weight creep test rig. All experiments are performed in a climate chamber at ambient temperature and 62.5% relative humidity over a period of 160 h. The neat matrix material is tested in one direction only whereas the LFT material is tested within and perpendicular to the flow direction. The UD material is tested within and perpendicular to its fiber direction as well as under 45° to the fiber direction to gain information about creep effects in shear dominated loading situations. For parameter identification and validation purposes, all experiments are simulated numerically by means of the finite element method using the material models proposed in Sect. 11.2.

11.3.2 Structural Experiments

For validation on the structural level, the proposed creep model is applied to the simulation of a load point support structure for thermoplastic sandwich structures designed in a previous study (Fliegener et al. [7]). The sandwich structure consists of two CFRP fase sheets with a symmetric $[0°, 90°, \pm45°]_s$ stacking sequence. The CFRP laminates are overmolded with a glass fiber reinfoced LFT ply on each side. In all instances, the same polyamide 6 based fiber reinforced materials as described in Subsect. 11.3.1 are employed. The face sheets are separated by a 20 mm thick thermoplastic PUR foam core. The sandwich plate is supplied with a loading point formed by a brass insert with a screw thread. To distribute the load smoothly from the brass insert into both face sheets, different types of load point support structues were investigated by Fliegener et al. [7]. The most promising support structure prooved to be the structure presented in Fig. 11.2. The support structure consists of the same LFT material as the LFT plies on top and bottom of the face sheets and is co-molded with the face sheets in a compression molding process.

For the numerical analysis, the breadboard specimen is meshed with standard displacement based finite elements considering a circular section of the square plate (Fliegener et al. [7], [8]). For the load point support structure and other LFT ranges as well as for the core, 8-node volume elements with tri-linear shape functions are used. For the CFRP laminate, 4-node first order shell elements are employed. The connection between volume and shell elements is made via appropriate constraint conditions. For a proper connection between all ranges, some triangular and tetrahedarl elements need to be used in addition. The finite element model of the breadboard specimen is modelled as clamped all around its external edges. It is loaded by a constant force

Fig. 11.2 Breadboard sandwich specimen with central load point and LFT load point support structure for validation on structural level.

acting in the downward normal direction. Due to the high stiffness of the panel, the analysis is performed within the geometrically linear framework.

The analysis is complemented by an experimental investigation, where breadboard specimens as presented in Fig. 11.2 are tested under different creep loads. The experiments are performed using a clamping system where the square specimen is placed into a tightly fitting box with a circular cutout with the same radius as the outer radius of the finite element model, thus providing similar external boundary conditions. Subsequently, a constant long term load is applied to the load point using an electromechanical Hegewald & Peschke inspekt table 250 testing machine. During the long term experiment, the crosshead displacement is continuously recorded. Since the load is constant, no strain variations in the loading rig and the machine's frame occur during the test so that crosshead displacement variations coincide with the displacement variations of the specimens load point due to creep.

11.4 Multiscale Simulation

As an additional approach for validation, a multiscale analysis is performed for the LFT material to predict the material response on the effectve level and to validate it against the experimental data available on coupon experiments. For this purpose, a representative volume element for the LFT microstructure is generated, employing the procedure presented earlier by Fliegener et al. [14]. The representative volume element is meshed using standard displacement based tetrahedral finite elements using the isotropic creep material model from Subsect. 11.2.2 for the matrix and assuming linear isotropic elasticity for the glass fibers with data sheet values for the Young's modulus and the Poisson's ratio. The finite element model is then subjected to a constant effective stress. The effective creep strain is computed as a function of time. By this means, numerical experiments for the LFT creep response on the macroscopic material level can be performed. The results are validated against the results of the physical laboratory experiments.

11.5 Results

11.5.1 Parameter Identification on Coupon Experiments

In a first validation step, the creep response of the neat matrix material is investigated. Uniaxial tensile loads of 5, 10, 15 and 20 MPa respectively are applied. The resulting creep curves are presented in Fig. 11.3 together with their counterparts obtained by a numerical simulaion based on the isotropic version (11.6) of the material model.

For all applied stress levels, the standard characteristics of the creep curves are observed. In the initial phase, a primary creep range with initially large creep rates

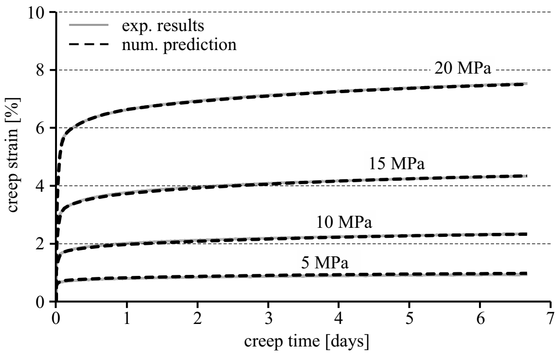

Fig. 11.3 Neat matrix material – experimental creep curves and numerical prediction by proposed viscoelastic material law.

is obtained. Subsequently, the creep rate decreases and the creep curves approach the secondary creep range featuring a constant creep rate. For all load levels, the material parameters in Eqs. (11.6) to (11.12) can be chosen such that the numerically predicted creep curves are in perfect agreement with their experimental counterparts, giving evidence for the rationale of the mathematical formulation of the constitutive model.

The isotropic viscoelastic material model with the material parameters determined before is then employed in a multiscale and homogenization analysis of the LFT material. The creep curves predicted by the multiscale analysis and the experimental counterparts for the LFT material are presented in Fig. 11.4, together with numerical predictions of the creep response using the anisotropic version (11.15) for the discontinuosly fiber reinforced LFT material with a parameter set fitted on this level of structural hierarchy. Both, the flow direction and the test direction perpendicular to the flow direction are considered.

Due to the discontinuous reinforcement by the linear elastic, non-viscous glass fibers, much lower creep strains are observed for the LFT material than for the neat matrix material, although the basic characteristics of the creep curves are maintained (see Figs. 11.3 and 11.4). For the tests within the flow direction, a rather good agreement of both numerical simulations – multiscale analysis and analysis based on the proposed LFT material model (11.15), respectively – with the experimental results is observed. Similar findings are obtained for the creep experiments perpendicular to the flow direction at the lower load levels. For the highest creep load level of 24 MPa, the proposed LFT creep model (11.15) and the experimental creep results are still found in a good agreement whereas the multiscale simulation slightly overestimates the creep rate in the initial phase, resulting in an overestimation of the creep strain in the entire creep period. This effect is probably caused by a suboptimal assumption on the fiber length and orientation distribution in the underlying representative volume element.

The results of the parameter identification for the continuously unidirectionally (UD) fiber reinforced material are presented in Fig. 11.5. The creep response is investigated within the fiber direction (0°), perpendicular to the fiber direction (90°) as well as under 45° to the fiber direction. Since the linear elastic carbon fibers carry

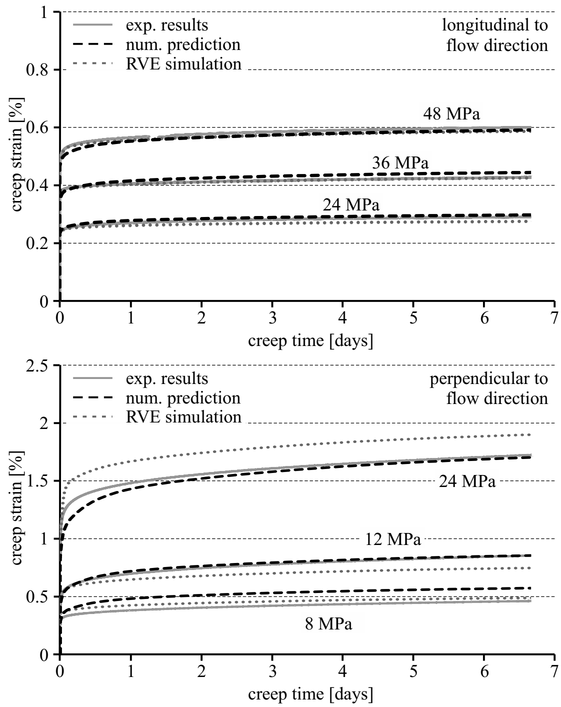

Fig. 11.4 Long fiber reinforced thermoplastics (LFT)–experimental creep curves, numerical prediction by proposed viscoelastic material law and results of multiscale analysis longitudinal and perpendicular to the flow direction.

almost the entire load within the fiber direction, almost no creep deformation develops in the experiment in the 0°-direction even under a higher load level. Perpendicular to the fiber direction and under 45° to the fiber direction, non-negligible creep effects are observed. Even for the UD CFRP material, creep effects are present when loaded in interfiber normal (90°) and shear modes (45°). Again, the experimental findings are found in a good agreement with the numerical simulation based on the proposed material model. Thus, also the UD version (11.13) of the creep model proves to provide a meaningful description of the macroscopic creep response if appropriate material parameters are selected.

Further experimental and numerical results are provided in the original publication (Fliegener and Hohe [8]).

11.5.2 Validation on Structural Level

For a validation of the proposed constitutive creep models for both LFT and UD composites together with the material parameters determined in Subsect. 11.5.1 under more complex multiaxial stress situations, the proposed material models are applied to a numerical simulation of the breadboard experiments on the load point support structure presented in Fig. 11.2.

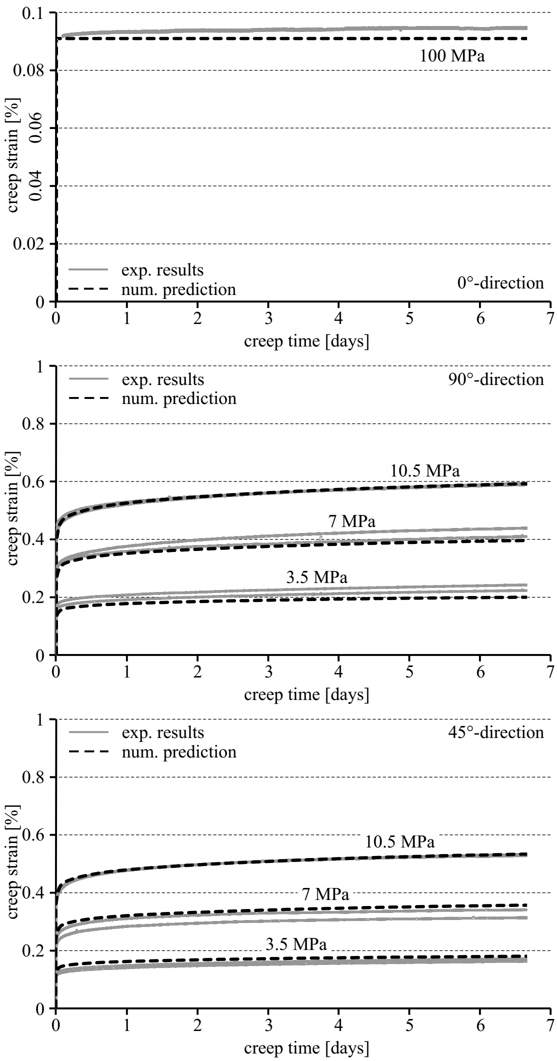

Fig. 11.5 Unidirectionally (UD) fiber reinforced thermoplastics – experimental creep curves and numerical prediction by proposed viscoelastic material law in 0°-, 90°- and 45°-direction to the fiber orientation.

The experimental and numerical results are presented in Fig. 11.6. In the first subfigure, the stress distribution in the LFT ranges of the overmolded LFT layers on top and bottom of the CFRP laminates forming the face sheets as well as in the co-molded load point support structure are shown. The second subfigure is concerned with the creep curves in terms of the crosshead (or load point) displacement as a function of time. Two different load levels with applied forces of 2.5 kN and 5 kN are investigated.

For both load levels, the experimentally observed and the numerically predicted creep curves are found in a good agreement, especially when considering the complexity of the underlying geometry and the complex creep problem involving both,

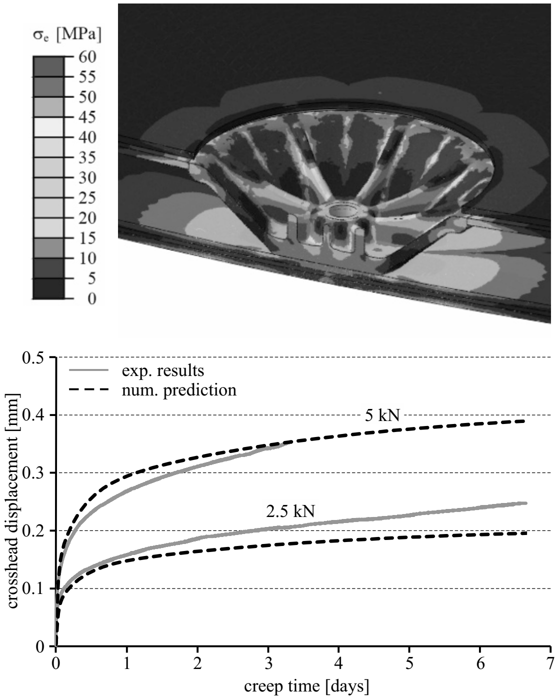

Fig. 11.6 Sandwich load point support structure – stress distribution in LFT material ranges as well as experimental creep curves and numerical prediction using proposed viscoelastic material law for the different material ranges.

UD CFRP laminates and glass fiber reinfoced LFT materials. Although the support structure design considered here proved to be the strongest among all optinons considered in the design study by Fliegener et al. [7] with a static failure load of 16.9 MPa, a significant amount of overall creep deformation is observed even at load levels of approximately 30% of the static failure load. Creep strains are found to develop especially in the co-molded LFT load point support structure and in the adjacent LFT plies on the inner side of the face sheets. Nevertheless, creep deformation is also observed in the UD plies of the face sheets, although limited to smaller amounts. The numerical simulation provides a good approximation of the experimental results, demonstrating the capabilities of the different versions of the proposed anisotropic constitutive model.

Further validations of the proposed material model on other types of load point support structures are presented in an earlier contribution by the present authors (Fliegener and Hohe [8]).

11.6 Summary and Conclusion

The present study is concerned with creep material models for fiber reinforced thermoplastics. Both, discontinuously and continuously fiber reinforced materials are considered. Based on an isotropic three element Kelvin-Voigt model, two different anisotropic versions are derived. Whereas the anisotropy for the discontinuously fiber reinforced material is introduced by introduction of anisotropy factors into the isotropic base formulation, fiber effects in the continuously finber reinforced material are introduced by superposition of the isotropic viscoelastic model representing the matrix with the anisotropic Hooke's law representing the effect of the fibers.

The model is validated against an experimental data base on coupon specimens concerning neat PA6, discontinuously long glass fiber reinforced thermoplastics and unidirectionally carbon fiber reinforced PA6 tape material. The experiments on laboratory specimens are complemented by experiments on more complex breadboard type sandwich specimens with central loading points. In all experiments on coupon and structural level, a good agrement of experimental and numerical data is observed.

The validated anisotropic material model proposed in the present study proves to provide a reliable tool for the numerical simulation of creep in glass or carbon fiber reinforced thermoplastics and structures made thereof. Both, continuously and discontinuously fiber reinforced microstructures as well as hybrid composites can be addressed. Although the development of substantial creep deformation is more likely for discontinuously fiber reinforced types, laminates consisiting of unidirectionally fiber reinforced plies might also experience non-negligible amounts of creep.

Acknowledgements The present contribution has been funded by the German Federal Department of Education and Research (BMBF) under grant no. 03X3041P as part of the collaborative "SMiLE" project. The authors are fully responsible for the contents of this contribution. The financial support is gratefully acknowledged. The authors wish to express their thanks to BASF and Fraunhofer ICT for provision of the material for the experimental studies.

References

[1] Bijsterbosch H, Gaymans RJ (1995) Polyamide 6—long glass fiber injection moldings. Polymer Composites **16**(5):363–369

[2] Henning F, Ernst H, Brüssel R (2005) LFTs for automotive applications. Reinforced Plastics **49**(2):24–33

[3] Chevali VS, Dean DR, Janowski GM (2009) Flexural creep behavior of discontinuous thermoplastic composites: Non-linear viscoelastic modeling and time–temperature–stress superposition. Composites Part A: Applied Science and Manufacturing **40**(6):870–877

[4] Greco A, Musardo C, Maffezzoli A (2007) Flexural creep behaviour of PP matrix woven composite. Composites Science and Technology **67**(6):1148–1158

[5] Brinson L, Knauss W (1991) Thermorheologically complex behavior of multiphase viscoelastic materials. Journal of the Mechanics and Physics of Solids **39**(7):859–880

[6] Schapery RA (1969) On the characterization of nonlinear viscoelastic materials. Polymer Engineering & Science **9**(4):295–310

[7] Fliegener S, Rausch J, Hohe J (2019) Loading points for industrial scale sandwich structures – A numerical and experimental design study. Composite Structures **226**:111,278

[8] Fliegener S, Hohe J (2020) An anisotropic creep model for continuously and discontinuously fiber reinforced thermoplastics. Composites Science and Technology **194**:108,168

[9] Fliegener S, Hohe J, Gumbsch P (2016) The creep behavior of long fiber reinforced thermoplastics examined by microstructural simulations. Composites Science and Technology **131**:1–11

[10] Haj-Ali RM, Muliana AH (2004) Numerical finite element formulation of the Schapery non-linear viscoelastic material model. International Journal for Numerical Methods in Engineering **59**(1):25–45

[11] N N (2003) ISO 3167: Plastics – multipurpose test specimens. Beuth, Berlin

[12] N N (2010) ISO 527-5: Plastics – determination of tensile properties – Part V: Test conditions for unidirectional fibre-reinforced plastic composites. Beuth, Berlin

[13] N N (2003) ISO 899-1: Plastics – determination of the creep behaviour – Part I: Tensile creep. Beuth, Berlin

[14] Fliegener S, Luke M, Gumbsch P (2014) 3D microstructure modeling of long fiber reinforced thermoplastics. Composites Science and Technology **104**:136–145